

## Relative Strengths of Fundamental and Harmonic Emissions of Solar Radio Type II Bursts

Rishikesh G. Jha<sup>1</sup> · K. Sasikumar Raja<sup>1</sup> ·  
R. Ramesh<sup>1</sup> · C. Kathiravan<sup>1</sup> · Christian  
Monstein<sup>2</sup>

© The author(s)

**Abstract** Solar radio type II bursts are slow-drifting bursts that exhibit various distinct features such as Fundamental (F) and Harmonic (H) emissions, band-splitting, and discrete fine structures in the dynamic spectra. Observationally, it has been found that in some cases the F emission is stronger than the H emission, and vice versa. The reason for such behavior has not been thoroughly investigated. To investigate this, we studied 58 meter wave (20-500 MHz) type II solar radio bursts showing both F and H emissions, observed during the period from 13 June 2010 to 25 December 2024, using data obtained with the Compound Astronomical Low frequency Low cost Instrument for Spectroscopy and Transportable Observatory (CALLISTO) spectrometers at different locations and Gauribidanur LOW-frequency Solar Spectrograph (GLOSS). We examined the intensity ratios of the H ( $I_H$ ) and F ( $I_F$ ) emissions and analyzed their variation with heliographic longitude. We found that 14 out of 19 bursts originating from heliographic longitudes beyond  $\pm 75^\circ$  exhibited an  $I_H/I_F$  ratio greater than unity. In contrast, 32 out of 39 bursts originating from longitudes within  $\pm 75^\circ$  showed a intensity ratio less than unity. From these results, we conclude that the relative strength of the F and H emissions can be influenced by refraction

---

✉ K. Sasikumar Raja  
[sasikumar.raja@iiap.res.in](mailto:sasikumar.raja@iiap.res.in)  
Rishikesh G. Jha  
[rishikesh.govind@iiap.res.in](mailto:rishikesh.govind@iiap.res.in)  
R. Ramesh  
[ramesh@iiap.res.in](mailto:ramesh@iiap.res.in)  
C. Kathiravan  
[kathir@iiap.res.in](mailto:kathir@iiap.res.in)  
C. Monstein  
[christian.monstein@irsol.usi.ch](mailto:christian.monstein@irsol.usi.ch)

<sup>1</sup> Indian Institute of Astrophysics, Koramangala-560 034, Bengaluru, India

<sup>2</sup> Istituto ricerche solari Aldo e Cele Dacco' (IRSOL), Universita' della Svizzera italiana, Locarno, Switzerland

due to density gradient in the solar corona, directivity and viewing angle of the bursts.

**Keywords:** Solar radio bursts, Type II bursts, Plasma emission, Shock waves, Fundamental and Harmonic emissions, Solar corona

## 1. Introduction

Solar Radio Bursts (SRBs) are broadly classified into five classes namely type I, type II, type III, type IV and type V based on their morphology and drift rates as observed from the dynamic spectrograms (time-frequency maps). Among them type II bursts are signatures of magnetohydrodynamic (MHD) shocks that occur in the solar corona, typically triggered by transient events such as Coronal Mass Ejections (CMEs) and flares (Payne-Scott, Yabsley, and Bolton 1947; Nelson and Robinson 1975; Mann, Classen, and Aurass 1995; Aurass 1997; Gopalswamy 2006; Gopalswamy et al. 2013; Nindos et al. 2011; Ramesh et al. 2012). In dynamic radio spectra, type II bursts appear as narrow band features that drift from high to low frequencies at a rate of approximately  $1 \text{ MHz s}^{-1}$ . These bursts are observed from meter wavelengths down to Deca-Hectometer (DH) and kilometer (KM) wavelengths. Type II bursts observed above  $3 R_{\odot}$  are generally referred to as interplanetary Type II bursts (Gopalswamy 2006).

It is known that type II bursts originate via the plasma emission mechanism. Firstly, a shock triggered by either CMEs or flare-associated blast waves excites plasma oscillations, called Langmuir oscillations, which are subsequently converted into electromagnetic waves through non-linear processes (McLean and Labrum 1985). Furthermore, some type II bursts exhibit both fundamental (F) and harmonic (H) structures (Wild, Murray, and Rowe 1954; Ganse et al. 2012; Kontar et al. 2017; Morosan et al. 2023). The frequency ratio between F and H emissions varies from 1.6 to 2.2, with a mean value of 1.8. In certain cases, second and third harmonic emissions have also been observed (Bacchini and Philippov 2024). Additionally, both F and H emissions may further split into a pair of bands, a phenomenon known as band splitting, which was first reported by Wild, Murray, and Rowe (1954). Type II bursts may also exhibit discrete sources or fragmentation, likely caused by turbulence and inhomogeneities in the ambient medium (Carley et al. 2021; Ramesh, Kathiravan, and Kumari 2023).

Observationally, it is known that the intensity densities of both the fundamental (F) and harmonic (H) emissions of type II bursts vary from burst to burst. For instance, in some cases, the F emission is stronger, while in others, the H emission dominates. In yet other cases, both have more or less the same intensity. In this article, we attempt to understand the reasons behind such intensity variations in F and H emissions.

**Table 1.** Locations of the spectrometers and frequency range.

S.No.	Station	Latitude (deg)	Longitude (deg)	Frequency Range (MHz)
1	ALASKA-COHOE	N60	W151	10–85
2	ALASKA-HAARP	N62	W145	10–85
3	Arecibo-Observatory	N18	W66	15–85
4	GREENLAND	N66	W50	10–110
5	BIR	N53	W8	10–100
6	ALGERIA-CRAAG	N36	E3	50–160
7	AUSTRIA-Krumbach	N47	E10	50–450
8	GERMANY-DLR	N53	E13	10–80
9	EGYPT-Alexandria	N31	E30	10–90
10	INDIA-OOTY	N11	E77	50–160
11	Gauribidanur-GLOSS	N14	E78	40–440
12	INDIA-GAURI	N14	E78	50–170
13	SSRT	N52	E102	50–425
14	Australia-ASSA	S35	E140	15–85

## 2. Observations

We used the type II solar radio bursts that are observed with e-CALLISTO spectrometers<sup>1</sup>, a network of radio spectrometers installed and operated over different longitudes to monitor the solar radio emission continuously (Benz et al. 2009; Monstein, Csillaghy, and Benz 2023). In addition, observations with GLOSS (Kishore et al. 2015) were also used for the present work<sup>2</sup>. The list of stations, their longitudes and latitudes, and operating frequency range are shown in Table 1.

We selected 58 type II bursts which has both F and H emissions from 13 CALLISTO spectrometers and GLOSS. For those events, the start time, start frequency of F and H emissions, amplitude/intensity (in dB) for F emission ( $I_F$ ) and H emissions ( $I_H$ ), heliographic longitude, heliographic latitude, active region number and flare class etc were obtained using the CALLISTO spectrometer observations as well as using publicly available CDAW<sup>3</sup> and Solar Monitoring<sup>4</sup> databases and the details are tabled in Table 2.

In Figure 1, upper panel shows type II burst in which fundamental emission was stronger and harmonic was weaker. This event was observed on 2023 October 26. This event occurred from an active region AR3473 located at heliographic

<sup>1</sup><https://www.e-callisto.org/>

<sup>2</sup><https://www.iiap.res.in/centers/gro/grids>

<sup>3</sup>[https://cdaw.gsfc.nasa.gov/CME\\_list/](https://cdaw.gsfc.nasa.gov/CME_list/)

<sup>4</sup><https://solarmonitor.org/>

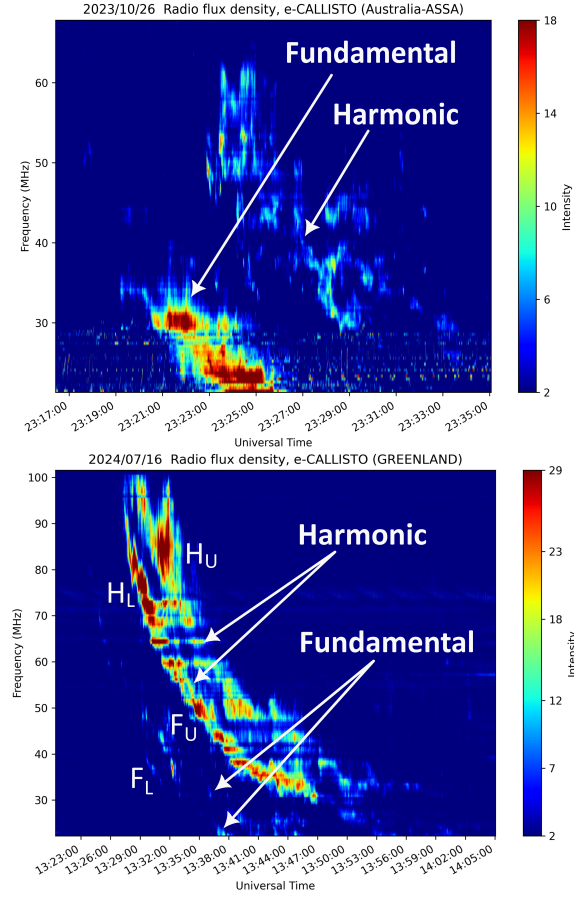


**Figure 1.** F and H emissions of type II bursts. In upper panel F emission is stronger than the H emission. In the lower panel H emission is stronger compared to the F emission. The lower panel also shows the band splitting phenomenon. Note that the different band-split lanes are indicated as  $F_U$ ,  $F_L$ ,  $H_U$ ,  $H_L$ .

longitude E30 and latitude N17. This event was associated with an X-ray flare of GOES class C1.4. Further in the lower panel shows another type II burst observed on 2024 July 16 using the CALLISTO spectrometer located at Greenland station. It is evident that F emission is weaker compared to the H emission. Further it is seen clearly the band splitting of F and H emissions. This event was associated with an active region AR3738 located at heliographic longitude W85 and latitude S06. This event was associated with an X-ray flare of GOES class X1.9. Similarly we have identified 58 type II bursts with F and H emission observed by various stations shown in Table 2.

### 3. Results and Discussions

In this work, we selected 58 type II bursts that exhibit both fundamental (F) and harmonic (H) emissions. We measured the intensities of both F and H emissions at a given time. These values were initially in dB scale. After converting them to a linear scale, we calculated the ratio  $I_H/I_F$ . Like wise, for every event, we measured the ratio at multiple epochs in the burst and the average value is considered. The use of intensity ratios, particularly the average value as mentioned above, has minimized the measurement errors. Additionally, we measured various observational parameters such as start time, start frequency, drift rates, frequency and intensity ratios of the H and F emissions, heliographic coordinates, active region numbers, flare class, etc. These parameters are tabulated in Table 2.

**Table 2.:** Details of the type II bursts observed.  $f_s$  - start frequency of the burst,  $V_D (= \Delta f / \Delta t)$  - drift rate of the burst where  $\Delta f$  is the band-width of burst and  $\Delta t$  is the duration of burst,  $f_H/f_F$  - frequency ratio of harmonic and fundamental emission,  $I_H/I_F$  - intensity ratio of the harmonic and fundamental emission.

Date	Station Name	Start Time	$f_s$ (MHz)	$V_D$ (MHz $s^{-1}$ )	$f_H/f_F$	$I_H/I_F$	Location	Active region	Flare class
13-06-2010	Gauribidanur-GLOSS	05:39	140	0.17	1.89	3.08	S25W84	AR1079	M1.0
04-09-2011	Gauribidanur-GLOSS	04:42	47	0.13	1.83	0.78	N19W67	AR1286	C9.0
02-05-2013	Gauribidanur-GLOSS	05:06	49	0.08	2.03	0.84	N10W26	AR1731	M1.1
05-11-2014	Gauribidanur-GLOSS	09:45	80	0.08	1.88	1.09	N20E68	AR2205	M7.9
09-10-2021	Australia-ASSA	06:34	71	0.07	1.82	0.12	N17E09	AR2882	M1.6
02-11-2021	Australia-ASSA	02:22	33	0.05	1.93	0.44	N14E01	AR2891	M1.7
20-12-2021	BIR	11:26	88	0.07	1.88	0.68	S22W05	AR2908	M1.8
12-02-2022	INDIA-GAURI	08:33	308	0.17	1.84	1.78	S19W84	AR2939	M1.4
02-03-2022	GREENLAND	17:38	101	0.10	1.72	3.76	N15E29	AR2958	M2.0
25-03-2022	Gauribidanur-GLOSS	05:14	74	0.20	2.03	0.41	S21E36	AR2974	M1.4
02-04-2022	GREENLAND	13:23	64	0.08	1.91	0.21	N15W61	AR2976	M3.9
17-04-2022	INDIA-OOTY	03:28	368	0.42	1.87	1.41	N12E88	AR2994	X1.1
30-04-2022	Arecibo-Observatory	13:46	81	0.09	1.96	1.26	N16W88	AR2994	X1.1
30-04-2022	ALASKA-HAARP	19:47	63	0.08	1.70	2.00	N16W88	AR2994	M1.9
04-07-2022	GREENLAND	13:32	86	0.07	1.90	0.04	N18E37	AR3050	C5.1
23-09-2022	Arecibo-Observatory	18:02	54	0.19	1.64	1.59	N19E77	AR3110	M1.7
29-09-2022	Arecibo-Observatory	12:00	83	0.05	1.77	1.12	N26E86	AR3107	C5.7
03-12-2022	Arecibo-Observatory	17:43	70	0.15	1.95	1.26	N14E89	AR3157	M1.2
20-01-2023	Arecibo-Observatory	14:01	85	0.08	1.78	0.41	S22W07	AR3190	C5.3
24-02-2023	ALASKA-HAARP	20:21	50	0.08	1.91	0.22	N29W24	AR3229	M3.7
03-03-2023	Arecibo-Observatory	18:05	76	0.02	1.72	1.13	N22W80	AR3234	X2.1
21-04-2023	Arecibo-Observatory	17:56	74	0.15	2.06	0.56	S22W11	AR3283	M1.7
04-05-2023	GERMANY-DLR	08:36	68	0.06	1.79	0.50	N17E43	AR3296	M3.9
06-05-2023	ALASKA-COHOE	00:47	54	0.09	1.62	0.57	N13E43	AR3297	C2.8
09-05-2023	SSRT	03:51	438	-1.02	1.77	0.11	N12W13	AR3296	M6.5
11-05-2023	INDIA-GAURI	08:57	160	0.12	1.66	0.79	S06W41	AR3294	M2.1
17-05-2023	Arecibo-Observatory	15:22	65	0.04	1.96	0.22	S18W45	AR3309	C4.3

*Continued on next page*

Continued from previous page

Date	Station Name	Start Time	$f_s$ (MHz)	$V_D$ (MHz/s)	$f_H/f_F$	$I_H/I_F$	Location	AR	Flare class
12-06-2023	INDIA-OOTY	07:02	82	0.10	1.93	0.11	N17W44	AR3330	C5.2
20-06-2023	Arecibo-Observatory	17:02	49	0.09	1.89	0.35	S17E73	AR3341	X1.1
02-07-2023	SSRT	02:34	211	0.62	1.67	0.79	S22E55	AR3359	M2.0
28-07-2023	ALASKA-HAARP	15:52	74	0.10	1.92	0.35	N27W87	AR3376	M4.1
17-08-2023	GERMANY-DLR	12:36	42	0.07	1.88	1.59	N19W80	AR3397	C5.1
26-08-2023	GREENLAND	12:56	58	0.07	1.88	2.51	N10W70	AR3405	C1.9
26-10-2023	Australia-ASSA	23:17	51	0.06	1.84	0.14	N17E30	AR3473	C1.4
29-01-2024	Australia-ASSA	04:11	85	0.05	1.84	1.12	N28W86	AR3559	M6.8
02-02-2024	Australia-ASSA	03:07	52	0.06	1.76	5.21	S18E60	AR3571	M1.1
07-02-2024	Australia-ASSA	03:21	83	0.03	2.00	0.11	S40W78	AR3575	M5.1
16-02-2024	Australia-ASSA	06:53	85	0.05	1.86	0.79	S16W80	AR3576	X2.5
10-03-2024	ALGERIA-CRAAG	12:10	151	0.11	1.98	0.45	S13W38	AR3599	M7.4
23-04-2024	GREENLAND	17:45	49	0.04	1.70	0.83	S08W59	AR3645	M2.9
08-05-2024	Australia-ASSA	05:09	33	0.05	1.80	0.50	S22W11	AR3664	X1.0
13-07-2024	GREENLAND	12:42	52	0.03	1.87	1.18	S08W42	AR3738	M5.3
16-07-2024	GREENLAND	13:23	94	0.06	1.85	4.48	S06W85	AR3738	X1.9
24-07-2024	GREENLAND	17:26	37	0.07	1.82	0.47	S07W71	AR3751	M2.9
29-07-2024	Gauribidanur-GLOSS	02:36	172	0.35	1.88	0.28	S05W04	AR3766	X1.5
05-08-2024	GREENLAND	15:30	53	0.05	1.91	0.20	S08E55	AR3780	X1.1
07-08-2024	GREENLAND	18:48	50	0.09	1.83	1.47	S07W07	AR3777	M5.0
01-10-2024	ALASKA-COHOE	22:17	73	0.06	1.90	0.16	S18E16	AR3842	X7.1
02-10-2024	Australia-ASSA	05:44	83	0.06	1.85	0.71	S15E20	AR3842	M3.6
03-10-2024	AUSTRIA-Krumbach	12:16	181	0.31	1.98	0.09	S15W03	AR3842	X9.0
09-10-2024	Australia-ASSA	01:45	42	0.09	1.98	0.22	N13W08	AR3848	X1.8
14-10-2024	ALASKA-HAARP	00:15	62	0.09	1.99	0.32	N10W78	AR3848	M3.4
25-11-2024	Australia-ASSA	20:43	69	0.10	1.96	1.26	N20E89	AR3908	M1.1
04-12-2024	INDIA-OOTY	10:04	86	0.12	1.70	5.01	S09E89	AR3917	M2.3
08-12-2024	INDIA-OOTY	09:04	119	0.12	1.85	4.47	S08W54	AR3912	X2.2
20-12-2024	EGYPT-Alexandria	10:13	140	0.21	1.71	0.35	S13E77	AR3932	C9.4
24-12-2024	INDIA-OOTY	08:41	149	0.09	1.98	0.25	S19E18	AR3932	M4.1
25-12-2024	SSRT	04:48	171	0.39	1.88	0.64	S18E06	AR3932	M4.9

In this study, we find that 58 type II bursts exhibit a systematic dependence of the harmonic-to-fundamental intensity ratio on the heliographic longitude, as shown in Figure 2. Among the 19 events located beyond heliographic longitudes of  $\pm 75^\circ$ , 14 (74%) exhibit a harmonic-to-fundamental intensity ratio  $I_H/I_F > 1$ . In contrast, among the remaining 39 events occurring within heliographic longitudes of  $\pm 75^\circ$ , 32 (82%) show a intensity ratio  $I_H/I_F < 1$ , suggesting dominant fundamental emission for disk events (see Table 3). There is no correlation between the flare class and the ratio  $I_H/I_F$ .

According to Caroubalos and Steinberg (1974), ground-based observations of type III radio bursts associated with sunspot regions located about  $70^\circ$  to either the east or west of the solar central meridian are predominantly harmonic (H) emission. The fundamental (F) component, however, shows a limiting directivity of  $\pm 65^\circ$  from the central meridian at 80 MHz (Suzuki and Sheridan 1982; Sasikumar Raja and Ramesh 2013). Furthermore, Morimoto et al 1963 suggests that

2/3 of intensity of type II bursts drops down for an angles between  $60^\circ - 90^\circ$ . Therefore we took average number  $75^\circ$  and a vertical line was drawn at  $75^\circ$  in Figure 2.

According to McLean and Labrum (1985) and Nelson and Robinson (1975), near the disk center the F emission usually exceeds the H emission in brightness. For events near or behind the limb the F emission is strongly attenuated by propagation effects due to density gradient in the corona.

Considering the close association between type II bursts and CMEs, we investigated the angular width of the CMEs associated with the type II bursts in our list. The mean angular width of the CMEs for the cases  $I_H/I_F > 1$  and  $I_H/I_F < 1$  are  $\approx 145^\circ$  and  $\approx 102^\circ$ , respectively. The maximum angular width of the CMEs for the case  $I_H/I_F < 1$  in our study is  $180^\circ$ . This implies that H emission is more intense than the F emission for wider CMEs.

Reports indicate a close association between the angular widths of the CMEs and the type II bursts. Wider CMEs have wider shocks and larger area where the electrons gain energy via shock acceleration (Michalek, Gopalswamy, and Xie 2007; Ramesh and Kathiravan 2022). CMEs/shocks with smaller radius of curvature are expected to be radio-quiet (Cairns et al. 2003). These results indicate that the probability of type II bursts occurring at locations other than the nose (leading edge) of the associated MHD shock is likely to be higher in the case of the wider CMEs. This is similar to the above mentioned discussion about type II bursts closer to the disk center and at the limb. So, it is possible that F emission can be more attenuated in the case of wider CMEs. It is known that radio bursts exhibit directional characteristics (Morimoto 1963; Steinberg, Caroubalos, and Bougeret 1974; Suzuki and Sheridan 1982; Ramesh, Kathiravan, and Satya Narayanan 2011; Ramesh et al. 2013; Mahender et al. 2020). Therefore, the chances of the observed variation in the intensities of the fundamental and harmonic emissions influenced by the directivity and the viewing angle too are there.

Note that directivity is defined as the ratio of the power received within a specified angular range from a source embedded in a scattering and refracting medium, to the power that would be received from the same source, at the same location and with the same total emitted power, if it were radiating isotropically in a vacuum (Thejappa, MacDowall, and Kaiser 2007).

The average drift rate and frequency ratio of the type II bursts in our study are  $\approx 0.13$  MHz/s and  $\approx 1.86$ , respectively. These are consistent with the similar values reported for type II bursts (Nelson and Melrose 1985; Mann, Classen, and Aurass 1995). There is east-west asymmetry in the locations of active regions associated with the type II bursts (Selvarani, Suresh, and Shanmugaraaju 2016).

In our study, we find that 24 events are from the East heliographic longitudes and 34 are observed from the Western heliographic longitudes. Further, all the events except one, originated from active regions located within the heliographic latitudes  $\pm 10^\circ - 30^\circ$ .

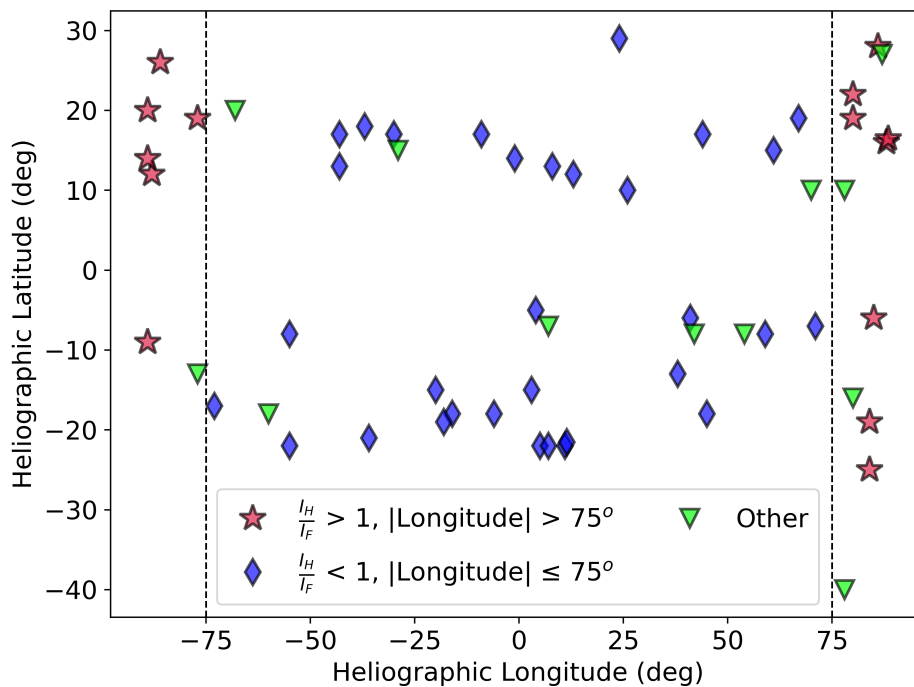


**Figure 2.** Location of the active regions associated with type II bursts. The blue diamonds indicate type II bursts that originated from and are associated with active regions whose longitudes are  $< 75^\circ$  and have  $I_H/I_F < 1$ . The red stars indicate type II bursts associated with active regions whose longitudes are  $> 75^\circ$  and have  $I_H/I_F > 1$ . The green diamonds indicate those that violate the conditions mentioned above.

**Table 3.** Statistics of type II bursts and their intensity ratios

Heliographic Longitude (L)	Number of Type II SRBs	$\frac{I_H}{I_F} > 1$	$\frac{I_H}{I_F} < 1$
$ L  > 75^\circ$	19	14	5
$ L  \leq 75^\circ$	39	7	32

#### 4. Summary

In this study, we explored 58 type II bursts that showed F and H emissions to understand large fraction  $\approx 64\%$  of type II bursts occur with strong F emissions and  $\approx 36\%$  of the bursts show strong H emissions. In some cases, both F and H emissions are nearly same. For this study we used the data obtained from CALLISTO spectrometers and GLOSS. We traced back to the activities from which type II bursts was originated using the existing catalogs mentioned previously. Our main results are:

- i) The bursts revealed a systematic dependence of the harmonic-to-fundamental intensity ratio of type II bursts on the heliographic longitude.
- ii) Among the 19 events located beyond heliographic longitudes of  $\pm 75^\circ$ , 14 (74%) exhibit a intensity ratio  $I_H/I_F > 1$ . This indicates that H emissions are stronger when the active region associated with type II bursts are located at heliographic longitudes greater than  $\pm 75^\circ$ .
- iii) Among 39 events occurring within  $\pm 75^\circ$ , 32 (82%) show  $I_H/I_F < 1$ . This indicates that F emissions are stronger when the active region associated with type II bursts are located at heliographic longitudes less than  $\pm 75^\circ$ .
- iv) The above results suggest that the observed relative variation in the intensities of the fundamental and harmonic emissions is a consequence of refraction due to density gradient in the solar corona, directivity and viewing angle of the bursts.
- v) Among the 58 type II bursts, 12 events differ from the above pattern. It is possible that the associated MHD shocks could have been non-radial for these events.

We intend to carry out a similar study with larger data set to verify the above results.

**Acknowledgements** We gratefully acknowledge the use of dynamic spectrogram data from the e-CALLISTO network stations: ALASKA-COHOE, ALASKA-HAARP, ALGERIA-CRAAG, Arecibo Observatory, Australia-ASSA, AUSTRIA-Krumbach, BIR, EGYPT-Alexandria, GERMANY-DLR, GREENLAND, INDIA-GAURI, INDIA-OOTY, and SSRT. We thank Indrajit V. Barve and G. V. S. Gireesh for discussions on the Gauribidanur-GLOSS data, and SolarMonitor.org team for providing details/images related to the different solar observations. We also acknowledge the use of SOHO/LASCO CME Catalog, generated and maintained at the CDAW Data Center by NASA and The Catholic University of America in cooperation with the Naval Research Laboratory. SOHO is a project of international cooperation between ESA and NASA. We thank anonymous referee for providing constructive comments and suggestions of the manuscript.

## References

- Aurass, H.: 1997, Coronal Mass Ejections and Type II Radio Bursts. In: Trotter, G. (ed.) *Coronal Physics from Radio and Space Observations* **483**, 135. DOI. ADS.
- Bacchini, F., Philippov, A.A.: 2024, Fundamental, harmonic, and third-harmonic plasma emission from beam-plasma instabilities: a first-principles precursor for astrophysical radio bursts. *Mon. Not. R. Astron. Soc.* **529**, 169. DOI. ADS.
- Benz, A.O., Monstein, C., Meyer, H., Manoharan, P.K., Ramesh, R., Altyntsev, A., Lara, A., Paez, J., Cho, K.-S.: 2009, A World-Wide Net of Solar Radio Spectrometers: e-CALLISTO. *Earth Moon and Planets* **104**, 277. DOI. ADS.
- Cairns, I.H., Knock, S.A., Robinson, P.A., Kuncic, Z.: 2003, Type II Solar Radio Bursts: Theory and Space Weather Implications. *Space Sci. Rev.* **107**, 27. DOI. ADS.
- Carley, E.P., Ceconi, B., Reid, H.A., Briand, C., Sasikumar Raja, K., Masson, S., Dorovskyy, V., Tiburzi, C., Vilmer, N., Zucca, P., Zarka, P., Tagger, M., Griebmeier, J.-M., Corbel, S., Theureau, G., Loh, A., Girard, J.N.: 2021, Observations of Shock Propagation through Turbulent Plasma in the Solar Corona. *Astrophys. J.* **921**, 3. DOI. ADS.
- Caroubalos, C., Steinberg, J.L.: 1974, Direct Measurements of the Directivity of Type I and Type III Radiation at 169 MHz (presented by C. Caroubalos). In: Newkirk, G.A. (ed.) *Coronal Disturbances, IAU Symposium* **57**, 239. ADS.

- Ganse, U., Kilian, P., Vainio, R., Spanier, F.: 2012, Emission of Type II Radio Bursts - Single-Beam Versus Two-Beam Scenario. *Sol. Phys.* **280**, 551. DOI. ADS.
- Gopalswamy, N.: 2006, Coronal Mass Ejections and Type II Radio Bursts. *Geophysical Monograph Series* **165**, 207. DOI. ADS.
- Gopalswamy, N., Xie, H., Mäkelä, P., Yashiro, S., Akiyama, S., et al.: 2013, Height of shock formation in the solar corona inferred from observations of type II radio bursts and coronal mass ejections. *Adv. Space Res.* **51**, 1981. DOI. ADS.
- Kishore, P., Ramesh, R., Kathiravan, C., Rajalingam, M.: 2015, A Low-Frequency Radio Spectropolarimeter for Observations of the Solar Corona. *Sol. Phys.* **290**, 2409. DOI. ADS.
- Kontar, E.P., Yu, S., Kuznetsov, A.A., Emslie, A.G., Alcock, B., Jeffrey, N.L.S., Melnik, V.N., Bian, N.H., Subramanian, P.: 2017, Imaging spectroscopy of solar radio burst fine structures. *Nature Communications* **8**, 1515. DOI. ADS.
- Mahender, A., Sasikumar Raja, K., Ramesh, R., Panditi, V., Monstein, C., Ganji, Y.: 2020, A Statistical Study of Low-Frequency Solar Radio Type III Bursts. *Sol. Phys.* **295**, 153. DOI. ADS.
- Mann, G., Classen, T., Aurass, H.: 1995, Characteristics of coronal shock waves and solar type II radio bursts. *Astron. Astrophys.* **295**, 775. ADS.
- McLean, D.J., Labrum, N.R.: 1985, Solar radiophysics : studies of emission from the sun at metre wavelengths. *Cambridge University Press*. ADS.
- Michalek, G., Gopalswamy, N., Xie, H.: 2007, Width of Radio-Loud and Radio-Quiet CMEs. *Sol. Phys.* **246**, 409. DOI. ADS.
- Monstein, C., Csillaghy, A., Benz, A.O.: 2023, *CALLISTO Quicklook Solar Spectrogram Plots*, International Space Weather Initiative. DOI. <https://spase-metadata.org/ISWI/DisplayData/Callisto/FAS/PT15M>.
- Morimoto, M.: 1963, On the Directivity of Solar Radio Bursts at Meter Waves. *Publ. Astron. Soc. Japan* **15**, 46. ADS.
- Morosan, D.E., Pomoell, J., Kumari, A., Kilpua, E.K.J., Vainio, R.: 2023, A type II solar radio burst without a coronal mass ejection. *Astron. Astrophys.* **675**, A98. DOI. ADS.
- Nelson, G.J., Melrose, D.B.: 1985, Type II bursts. *Cambridge University Press*, 333. ADS.
- Nelson, G.J., Robinson, R.D.: 1975, Multi-Frequency Heliograph Observations of Type II Bursts. *Proc. Astron. Soc. Aust.* **2**, 370. DOI. ADS.
- Nindos, A., Alissandrakis, C.E., Hillaris, A., Preka-Papadema, P.: 2011, On the relationship of shock waves to flares and coronal mass ejections. *Astron. Astrophys.* **531**, A31. DOI. ADS.
- Payne-Scott, R., Yabsley, D.E., Bolton, J.G.: 1947, Relative Times of Arrival of Bursts of Solar Noise on Different Radio Frequencies. *Nature* **160**, 256. DOI. ADS.
- Ramesh, R., Kathiravan, C.: 2022, New Results from the Spectral Observations of Solar Coronal Type II Radio Bursts. *Astrophys. J.* **926**, 38. DOI. ADS.
- Ramesh, R., Kathiravan, C., Kumari, A.: 2023, Solar Coronal Density Turbulence and Magnetic Field Strength at the Source Regions of Two Successive Metric Type II Radio Bursts. *Astrophys. J.* **943**, 43. DOI. ADS.
- Ramesh, R., Kathiravan, C., Satya Narayanan, A.: 2011, Low-frequency Observations of Polarized Emission from Long-lived Non-thermal Radio Sources in the Solar Corona. *Astrophys. J.* **734**, 39. DOI. ADS.
- Ramesh, R., Kathiravan, C., Anna Lakshmi, M., Gopalswamy, N., Umopathy, S.: 2012, The Location of Solar Metric Type II Radio Bursts with Respect to the Associated Coronal Mass Ejections. *Astrophys. J.* **752**, 107. DOI. ADS.
- Ramesh, R., Sasikumar Raja, K., Kathiravan, C., Narayanan, A.S.: 2013, Low-frequency Radio Observations of Picoflare Category Energy Releases in the Solar Atmosphere. *Astrophys. J.* **762**, 89. DOI. ADS.
- Sasikumar Raja, K., Ramesh, R.: 2013, Low-frequency Observations of Transient Quasi-periodic Radio Emission from the Solar Atmosphere. *Astrophys. J.* **775**, 38. DOI. ADS.
- Selvarani, G., Suresh, K., Shanmugaraju, A.: 2016, Investigation on the source location of flares associated with type II radio bursts using multi-wavelength observations. *Ind. J. Radio Space Phys.* **45**, 154. <http://nopr.niscares.in/handle/123456789/41332>.
- Steinberg, J.L., Caroubalos, C., Bougeret, J.L.: 1974, STEREO-1 measurements of the beam pattern of 169 MHz type I bursts on November 18, 1971. *Astron. Astrophys.* **37**, 109. ADS.
- Suzuki, S., Sheridan, K.V.: 1982, On the fundamental and harmonic components of low-frequency Type III solar radio bursts. *Proc. Astron. Soc. Aust.* **4**, 382. DOI. ADS.
- Thejappa, G., MacDowall, R.J., Kaiser, M.L.: 2007, Monte Carlo Simulation of Directivity of Interplanetary Radio Bursts. *Astrophys. J.* **671**, 894. DOI. ADS.

Wild, J.P., Murray, J.D., Rowe, W.C.: 1954, Harmonics in the Spectra of Solar Radio Disturbances. *Aust. J. Phys.* **7**, 439. [DOI](#). [ADS](#).